



## Summer upwelling frequency along the western Cantabrian coast from 1967 to 2007

I. Alvarez<sup>a,b,\*</sup>, M. Gomez-Gesteira<sup>a</sup>, M. deCastro<sup>a</sup>, J.L. Gomez-Gesteira<sup>c</sup>, J.M. Dias<sup>b</sup>

<sup>a</sup> EPhysLab (Environmental Physics Laboratory), Universidade de Vigo, Facultade de Ciencias, Ourense, Spain

<sup>b</sup> CESAM, Universidade de Aveiro, Departamento de Física, Aveiro, Portugal

<sup>c</sup> Area de Control y Gestion del Medio Marino y los Recursos Marinos, Fundacion CETMAR, Vigo, Spain

### ARTICLE INFO

#### Article history:

Received 18 May 2009

Received in revised form 8 September 2009

Accepted 21 September 2009

Available online 30 September 2009

#### Keywords:

Upwelling

Cantabrian coast

Ekman transport

SST

### ABSTRACT

Upwelling events have been analyzed along the western part of the Cantabrian coast from 1967 to 2007. This analysis shows that the highest number of days under upwelling favorable conditions was observed from June to September (12–14 days per month) with a probability of finding consecutive days under upwelling favorable conditions decreasing from 47% to 17% when events between 1 and 5 consecutive days were considered respectively. This situation was also corroborated by Sea Surface Temperature data which revealed the presence of cold water over the continental shelf, near coast, associated with upwelling favorable winds. This cold water was also observed inside the estuaries located in this area. The water temperature signal measured at the inner part of the Ria de O Barqueiro (NW Iberian Peninsula) from June to September 2008 showed to be negatively correlated with the Upwelling Index calculated in front of the northern Galician coast. This correlation tends to increase as the number of lag days between both variables increases. The maximum value of  $-0.8$  corresponds to a lag of 5 days.

© 2009 Elsevier B.V. All rights reserved.

### 1. Introduction

The understanding of the vulnerability and adaptation of some marine species to environmental changes constitutes an arduous task due to presence of different factors that can affect both positively and negatively the spreading of those species. In the particular case of the northwestern part of Iberian Peninsula (Fig. 1), differences in coastal temperatures between the Atlantic and Cantabrian coastline during summer (Fraga, 1981; Prego and Bao, 1997; Bode et al., 2002; Garcia-Soto et al., 2002; Torres et al., 2003; Alvarez et al., 2005) can provide different development conditions for many invasive alien species (IAS) from warmer waters. This is the case of the Pacific oyster (*Crassostrea gigas*) that although is cultured in the western Galician rias (south of Cape Finisterre) and spawning has been described in this area (Ruiz, et al., 1992), there is no evidence of a natural settlement of the larvae stage. On the contrary, naturalized populations of this species have been located in different areas of the Cantabrian shoreline. According to different authors (Mann et al., 1991; Shatkin et al., 1997) larval survival of Pacific oyster needs temperatures above 18° during at least 2 weeks in July and August. Thus, coastal upwelling can play a dual role since it provides the nutrients necessary for the development of marine species but, at the same time, it is responsible for sudden decreases in water temperature that can be potentially harmful for those species.

Several facts can be summarized from previous upwelling studies on both coasts. First, upwelling is mainly a spring–summer process, although some authors have also detected upwelling events in autumn–winter (Santos et al., 2001; Alvarez et al., 2003; Borges et al., 2003; Santos et al., 2004; deCastro et al., 2006a; Prego et al., 2007; deCastro et al., 2008a; Alvarez et al., 2009). Second, upwelled water is generally Eastern North Atlantic Central Water (ENACW; T–S definition can be found in Fiuzza, 1984 and Ríos et al., 1992) which is a cold and salty water mass. However, some authors have detected different upwelled waters associated with the Iberian Poleward Current (Alvarez et al., 2003; Prego et al., 2007) and with shelf bottom seawater (Alvarez et al., 2009). Third, upwelling frequency and intensity are influenced by coastal orientation (Torres et al., 2003; Gomez-Gesteira et al., 2006; Alvarez et al., 2008a) which modulates wind direction and intensity. As a result of this different coastal orientation, upwelling favourable conditions are prevalent in the spring–summer along the western coast but not along the northern one. Possibly, this is the reason why upwelling research has been mainly focused on the western coast. Thus, different features of northern coastal upwelling remain unknown and need to be answered, for example, to determine the commercial viability of invasive alien species. In particular, the historical frequency and intensity have not been studied so far using long term data series. As far as we know, only Llope et al. (2006) have analyzed the long term behavior of upwelling processes around Cape Peñas ( $\sim 5^\circ 51' W$ ,  $43^\circ 39' N$ ). Finally, the entrance of upwelled water into the inner part of the estuaries and its dependence on atmospheric forcing has still to be analyzed.

The aim of this manuscript is to analyze the influence of upwelling events along the western part of the Cantabrian coast. This study

\* Corresponding author. EPhysLab (Environmental Physics Laboratory), Universidade de Vigo, Facultade de Ciencias, Ourense, Spain.  
E-mail address: [ialvarez@uvigo.es](mailto:ialvarez@uvigo.es) (I. Alvarez).

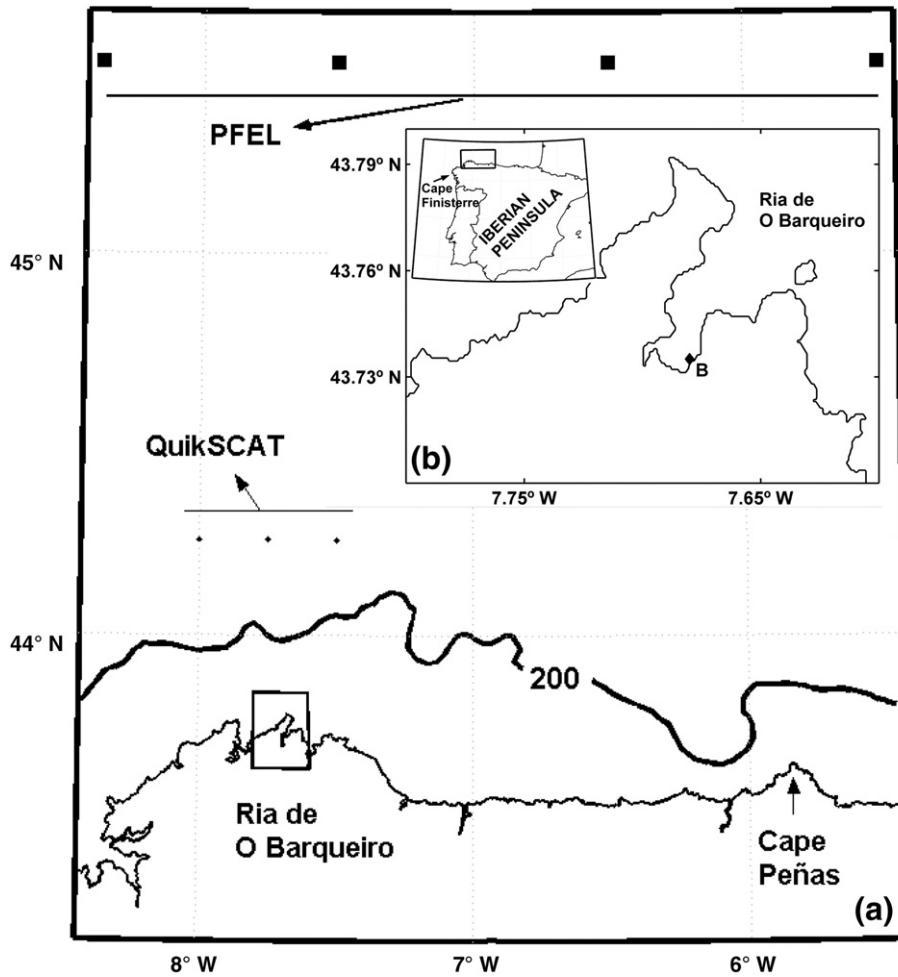


**Fig. 1.** (a) Map of the western Cantabrian coast. Black circles represent the 3 control points considered to analyze wind data provided by the QuikSCAT satellite and black squares represent the 4 points where Ekman transport data from the PFEL were obtained. (b) Map of the Ria de O Barqueiro showing the sampling hydrographic station (black diamond, st. B).

focuses on different spatio-temporal scale. On the one hand, the frequency and intensity of upwelling events will be described at shelf locations from 1967–2007 by means of Ekman volume transport and Sea Surface Temperature (SST). On the other hand, the dependence of SST on upwelling conditions will be studied in the inter-tidal area of a northern Galician ria for a continuous period (June–September 2008).

**2. Data and methods**

To analyze the occurrence of summer upwelling events over the last 41 years (1967–2007), Ekman transport data provided by the Pacific Fisheries Environmental Laboratory (PFEL) (<http://www.pfel.noaa.gov>) were used. The PFEL distributes environmental index products and time series data bases to cooperating researchers, taking advantage of its long association with the U.S. Navy's Fleet Numerical Meteorology and Oceanography Centre (FNMOC). FNMOC produces operational forecasts of the state of the atmosphere and the ocean several times daily and maintains archives of several important parameters. These parameters are model derived products which are routinely distributed to researchers. For our purposes six-hourly Ekman transport data model derived from Sea Level Pressure were considered at 4 selected longitudes (8.5°W, 7.5°W, 6.5°W, 5.5°W) along 45.5°N located in front of the area under study (Fig. 1(a), black squares) on an approximately 1° × 1° grid. These data sets were averaged to obtain daily series.

To analyze the wind patterns measured from June to September 2008, surface wind fields provided by the QuikSCAT satellite, and retrieved from the Jet Propulsion Laboratory web site ([http://podaac.](http://podaac.jpl.nasa.gov/DATA_CATALOG/quikscatinfo.html)

[jpl.nasa.gov/DATA\\_CATALOG/quikscatinfo.html](http://podaac.jpl.nasa.gov/DATA_CATALOG/quikscatinfo.html)) were used. The data set consists of global grid values of meridional and zonal components of wind measured twice daily on an approximately 0.25° × 0.25° grid with global coverage. QuikSCAT data are given in an ascending and descending pass. Data corresponding to one pass present numerous shadow areas, therefore, an average between both passes was considered to increase the coverage. Wind data from the near-coastal zone with offshore distances of about 25 km are not available due to the applied coast mask. Nevertheless, a statistical comparison between QuikSCAT wind measurements and high resolution numerical models was carried out along the Galician coast (Penabad et al., 2008), revealing similar results between models and satellite data. Ekman transport was calculated using the wind speed from the QuikSCAT satellite at 3 control points located along the northern Galician coast at latitude 44.25°N and from 7.5°W to 8°W (Fig. 1(a), black circles).

A practicable upwelling index (UI) results from the meridional component of the Ekman volume transport per unit length  $Q_y = -\frac{\rho_a C_d}{\rho_w f} (W_x^2 + W_y^2)^{1/2} W_x$  where  $W_x$ ,  $W_y$  are the zonal and meridional components of wind data,  $\rho_a = 1.22 \text{ kg m}^{-3}$  is the air density,  $C_d = 1.4 \times 10^{-3}$  is a dimensionless drag coefficient,  $\rho_w = 1025 \text{ kg m}^{-3}$  is the sea water density and  $f$  is the local Coriolis frequency (Bakun, 1973; Nykjaer and Van Camp, 1994; Gomez-Gesteira et al., 2006). The latter will be considered to be constant along the Cantabrian coast because it only slightly deviates from the pure west–east orientation. In fact, only along the northern Galician coast it is possible to observe an irregular coastline due to the presence of the northern Galician rias (Fig. 1(a)). Nevertheless, a recent study carried out by Gomez-Gesteira et al. (2006) using modeled wind data around the Galician

coast, showed that along the northern Galician coast ( $\sim 7.5\text{--}8.5^\circ\text{W}$ ) the wind direction presents the same behavior with some small differences in amplitude values. Thus, macroscopically the Cantabrian coast can be considered approximately parallel to the equator and the  $Q_y$  component can be considered as the UI. Positive (negative) UI values mean upwelling favorable (unfavorable) conditions.

The most representative teleconnection indices in the Northern Hemisphere (NAO, EA, SCA, EA/WR and POL) have been obtained from the Climate Prediction Center (CPC) at the National Center of Environmental Prediction (NCEP) at monthly time scales from 1967 to 2007. These modes have shown to be the most prevalent patterns on the eastern North Atlantic region (Rodríguez-Puebla et al., 1998; Lorenzo and Taboada, 2005; deCastro et al., 2006b). Although a detailed description of these teleconnection indices can be found on the web site from the NCEP (<http://www.cpc.noaa.gov>) a brief description will be given here. The North Atlantic Oscillation (NAO) consists of a north–south dipole of geopotential anomalies with one center located over Iceland and the other one spanning between  $35^\circ\text{N}$  and  $40^\circ\text{N}$  in the central North Atlantic. The East Atlantic (EA) pattern consists of a north–south dipole that spans the entire North Atlantic Ocean with the centers near  $55^\circ\text{N}$ ,  $20\text{--}35^\circ\text{W}$  and  $25\text{--}35^\circ\text{N}$ ,  $0\text{--}10^\circ\text{W}$ . The anomaly centers of the EA pattern are displaced southeastward to the centers of the NAO pattern. The Scandinavia pattern (SCA) consists of a primary circulation center over Scandinavia, with a weaker center of opposite sign over western Europe. The East Atlantic/West Russia (EA/WR) pattern is one of three prominent teleconnection patterns that affects Eurasia through the year. This pattern consists of four main anomaly centers. The Europe Polar/Eurasia pattern (POL) consists of one center over the polar region and centers of opposite sign over Europe and northeastern China.

Sea Surface Temperature (SST) data were obtained from the NOAA/NASA Advanced Very High Resolution Radiometers (AVHRR) (<http://poet.jpl.nasa.gov>). Data are available from 1985, and they are distributed in a variety of resolutions and temporal averages. In the present study a spatial resolution of 4 km and a temporal average of 8 days were considered. Each data product is obtained as either an ascending (daytime) or descending (night-time) image. Only the night-time image was considered to avoid the solar heating effect.

Water temperature was measured at the inner part of the Ria de O Barqueiro (Fig. 1(b), black diamond (st. B)) using a DST CTD (Data Storage Tag, Conductivity Temperature Depth) recorder. This is a compact microprocessor-controlled temperature, depth and conductivity with two conductivity cells, temperature and pressure sensors placed in the device cup. CTD is inserted into a plastic protective housing deployed approximately 0.5 m above the sea bed by using a metal trestle of the commercial oyster bag culture. The constant sampling interval of T and S was 1 h. Only temperature data will be considered in the present study due to the low accuracy of the conductivity cells to identify small changes in salinity. Note that the location of temperature recorder in the intertidal area (0.5 m to 4 m deep from low tide to high tide) was specially designed to identify upwelling induced changes in the area where commercial species as oysters are cultured.

### 3. Results and discussion

The study of upwelling effect on the northern coast of the Iberian Peninsula was carried out in terms of Upwelling Index from 1967 to 2007 and water temperature both at offshore locations and inside estuaries.

#### 3.1. Upwelling Index analysis

The time evolution of the UI from 1967 to 2007 was calculated taking into account 4 control points shown in Fig. 1(a) (black squares). The inter-annual evolution of UI (Fig. 2(a)) shows a marked annual cycle, with maximum values (upwelling favorable conditions) in July–August and minimum values in December–January. The monthly behavior associated with the annual cycle can be determined by averaging UI for each month during the period 1967–2007. This monthly average of UI (Fig. 2(b)) shows positive values from June to August at all points with the maximum values in July ( $\sim 300 \text{ m}^3 \text{ s}^{-1} \text{ km}^{-1}$ ). For the rest of the year UI shows negative values. Taking into account the small changes among the points located along the coast observed in Fig. 2(a, b) it is possible to consider a longitudinal average of UI. The inter-annual evolution of the longitudinal average of UI (Fig. 2(c)) shows maximum

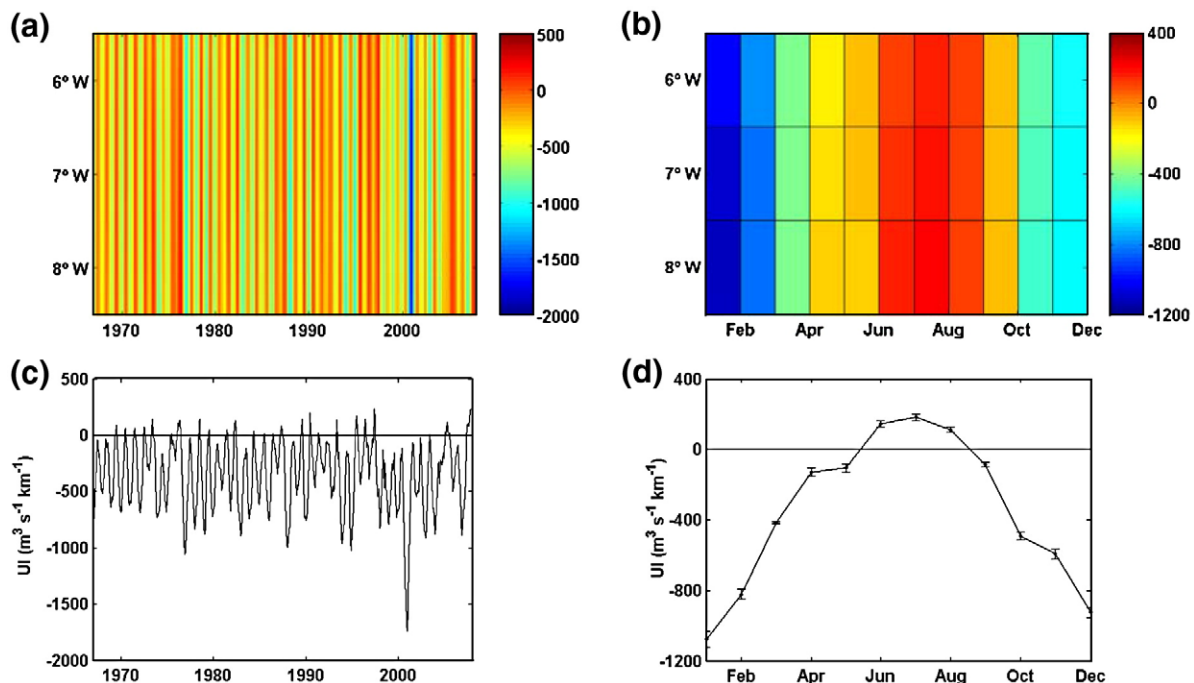


Fig. 2. (a) Inter-annual evolution of the Upwelling Index (UI) [ $\text{m}^3 \text{ s}^{-1} \text{ km}^{-1}$ ] from 1967 to 2007. (b) 41-year (1967–2007) mean of the annual evolution of UI. (c) Inter-annual evolution of the longitudinal average of UI from 1967 to 2007. (d) Annual cycle calculated by averaging UI in longitude and time from 1967 to 2007.

**Table 1**

Correlation coefficient between UI-winter (DJF) atmospheric patterns and UI-summer (JJA) atmospheric patterns from 1967 to 2007 at the 4 control points.

	8.5°W		7.5°W		6.5°W		5.5°W	
	DJF	JJA	DJF	JJA	DJF	JJA	DJF	JJA
NAO	−0.35*	0.29*	−0.34*	0.30*	−0.34*	0.31*	−0.33*	0.31*
EA	−0.47*	−0.43*	−0.45*	−0.43*	−0.43*	−0.42*	−0.39*	−0.39*
EA/WR	0.47*	–	0.48*	–	0.49*	–	0.51*	–

\* significance level &gt;95%.

values in July–August and minimum values in December–January. The longitudinal and time averaging of UI is represented in Fig. 2(d). The highest positive values ( $\sim 300 \text{ m}^3 \text{ s}^{-1} \text{ km}^{-1}$ ) are observed from June to August. Negative values can be observed for the rest of the year, showing unfavorable upwelling conditions during most of the year. The error bars were calculated using the standard deviation of the monthly data,  $\sigma(UI^W)$ . Error bars are observed to be negligible compared to the amplitude of the annual cycle, which ranges from  $-1200 \text{ m}^3 \text{ s}^{-1} \text{ km}^{-1}$  to  $300 \text{ m}^3 \text{ s}^{-1} \text{ km}^{-1}$ .

The observed seasonal cycle can be compared with that reported by Alvarez et al. (2008b) from the Iberian west coast (see Fig. 7 in that reference). Resulting patterns are very similar and exhibit positive peak values in summer, but negative ones in winter. Nevertheless, there are several significant differences among them. For instance, upwelling favorable conditions can be observed from March to September along the western coast but only from June to August along the northern coast. In addition, the highest values are close to  $800 \text{ m}^3 \text{ s}^{-1} \text{ km}^{-1}$  along the western coast and only close to  $300 \text{ m}^3 \text{ s}^{-1} \text{ km}^{-1}$  along the northern one.

Interannual changes of UI can be also analyzed in terms of the most representative atmospheric modes in the North Atlantic. Teleconnection patterns reflect large-scale changes in the atmospheric wave and jet stream patterns, which can influence temperature, rainfall, storm tracks, and/or jet stream location/intensity over vast areas. Thus, they are often the phenomenon responsible for abnormal weather patterns occurring simultaneously over seemingly vast distances. Previous studies (Rodríguez-Puebla et al., 1998; Lorenzo and Taboada, 2005; deCastro et al., 2006b) consider that the most representative regional patterns of atmospheric variation in the Northern Hemisphere with some influence on the eastern North Atlantic region are: NAO, EA, SCA, EA/WR and POL. The temporal variability of upwelling along the western Cantabrian coast can be analyzed taking into account the influence of these atmospheric patterns. Considering the observed behavior in Fig. 2(d), the monthly indices and UI were correlated considering the winter season from December to February and the summer season from June to August at the 4 control points (Table 1).

In winter, UI shows the highest correlation coefficient value for the EA/WR pattern with a significant positive correlation along the entire area (close to 0.5). A negative correlation can be also observed for the EA and NAO patterns with a correlation coefficient around  $-0.4$  and  $-0.3$  respectively. UI and the rest of atmospheric indices are not significantly correlated. Taking into account these values it is possible to observe that EA/WR and EA are the most important teleconnection patterns on UI variability although the NAO pattern also shows some influence.

The correlations obtained in summer show that the EA pattern is the most important mode. UI shows a negative correlation with the highest correlation coefficient around  $-0.4$  at the 4 control points. The NAO pattern also shows some influence on the UI with a positive correlation although the correlation coefficient value is on the order of 0.3. These results can be compared with that obtained by deCastro et al. (2008b) along the western coast of the Iberian Peninsula. They found that the main upwelling variability (considering the upwelling season as JASO) can be explained in terms of the EA pattern with a significant negative correlation (close to  $-0.4$ ) along the entire coast. NAO pattern was the second atmospheric mode with some influence on upwelling variability showing a significant positive correlation.

Upwelling prevalence can be studied both in terms of the mean number of days under upwelling favorable conditions and the probability of finding consecutive days under these upwelling favorable conditions. Actually, previous studies carried out at the western coast of the Iberian Peninsula proved that upwelled water can be easily identified when upwelling favorable conditions persist for more than 3–4 days (Alvarez-Salgado et al., 2000; Alvarez et al., 2005; Alvarez-Salgado et al., 2006). In addition, a recent study at the northern Galician coast (Alvarez et al., 2009) also characterized a winter upwelling event observed after 9 consecutive days of upwelling favorable conditions.

The mean number of days per month under favorable wind conditions ( $UI > 16 \text{ m}^3 \text{ s}^{-1} \text{ km}^{-1}$ ) was calculated from 1967 to 2007 at the 4 control points located along the Cantabrian coast (Fig. 1(a), black squares). For the sake of clarity only the 2 points (6.5°W and 7.5°W) located in the central part of the area were represented (Fig. 3(a)). Note that the threshold ( $16 \text{ m}^3 \text{ s}^{-1} \text{ km}^{-1}$ ) corresponds to weak winds ( $< 1 \text{ m s}^{-1}$ ) as well as to calms. The highest number of days was observed during the spring–summer months with 12–14 days per month, while during the autumn–winter period the number of days was lower (8–10 days per month) although not negligible (Alvarez et al., 2009). This situation can be also compared with the one observed at the western coast of the Iberian Peninsula (Cabanas and Alvarez, 2005; deCastro et al. 2008a). The highest number of days under upwelling favorable conditions along the western coast is also observed during the summer months although with higher values ( $\sim 22$ –25 days per month) than along the northern coast. During the winter period it is also possible to observe a number of days under favorable conditions along the western coast ( $\sim 10$ –12 days per month) higher than along the northern one.

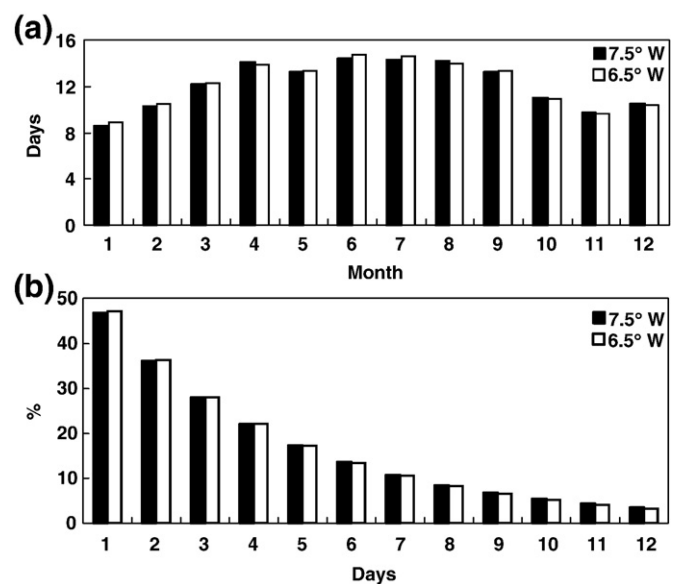


**Fig. 3.** (a) Number of days with  $UI > 16 \text{ m}^3 \text{ s}^{-1} \text{ km}^{-1}$  per month averaged from 1967 to 2007 and (b) Probability of finding consecutive days under upwelling favorable conditions ( $UI > 16 \text{ m}^3 \text{ s}^{-1} \text{ km}^{-1}$ ) in summer (June–September) from 1967 to 2007 at the control points 45.5°N, 7.5°W and 45.5°N, 6.5°W (black squares in Fig. 1(a)).

Taking into account the previous results it is possible to conclude that the summer season is characterized by exceptionally favored coastal upwelling conditions. Upwelling duration was also analyzed at the same control points from June to September. Fig. 3(b) shows the probability of finding consecutive days under upwelling favorable conditions ( $UI > 16 \text{ m}^3 \text{ s}^{-1} \text{ km}^{-1}$ ) from 1967 to 2007. The highest probabilities can be found between 1 and 5 consecutive days reaching values of 47% and 17% respectively.

In addition to the upwelling duration, the mean intensity of UI was also analyzed during these months taking into account the intensity values corresponding to the days under upwelling favorable conditions. Fig. 4(a) shows  $\langle UI \rangle^F$  average calculated from June to September for each year at the 2 control points, where the superscript  $F$  refers to the fact that averaging was performed considering only the days under upwelling favorable conditions ( $UI > 16 \text{ m}^3 \text{ s}^{-1} \text{ km}^{-1}$  as shown above). A 2-year running average was considered for each point to better show the overall behavior. UI has a similar pattern at both control points although the westernmost point ( $7.5^\circ \text{W}$ , solid line) presents intensity values slightly higher than the other point throughout the whole period. Straight lines represent a linear fit to better observe the general trends. The upwelling intensity tends to

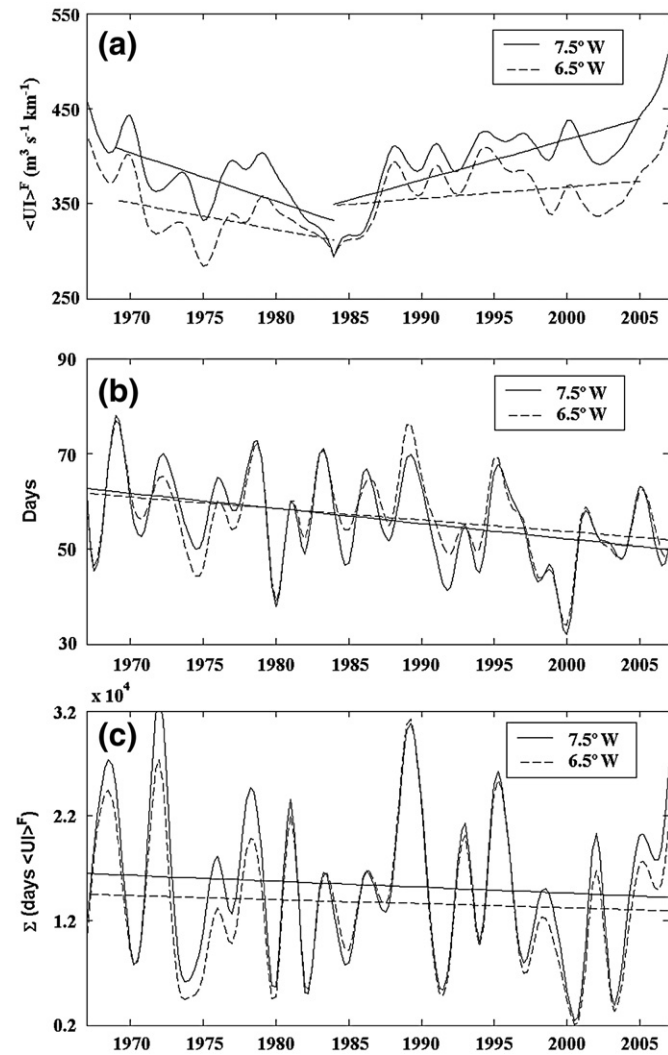


Fig. 4. (a) Annual upwelling intensity ( $\text{m}^3 \text{ s}^{-1} \text{ km}^{-1}$ ) averaged from June to September (1967–2007). (b) Number of days per year under upwelling favorable conditions from June to September (1967–2007). (c)  $\sum_{i=1}^N n_i \langle UI \rangle_i^F$  where  $n_i$  is the number of consecutive days under upwelling favorable conditions with  $n_i \geq 3$ ,  $\langle UI \rangle_i^F$  is the mean intensity of UI during these days and  $N$  is the number of events per year. Straight lines in each frame show the linear fit at the two control points.

decrease from the beginning of the period to 1984 and increases from 1984 on at both points. To analyze trends the original data were considered instead of the 2-year running average. During the decrease period (1969–1984) the upwelling intensity at each point shows a negative trend with values of  $-6 \text{ m}^3 \text{ s}^{-1} \text{ km}^{-1} \text{ yr}^{-1}$  at  $7.5^\circ \text{W}$  and  $-4 \text{ m}^3 \text{ s}^{-1} \text{ km}^{-1} \text{ yr}^{-1}$  at  $6.5^\circ \text{W}$ . From 1984 to 2005, intensity shows a positive trend with values of  $6 \text{ m}^3 \text{ s}^{-1} \text{ km}^{-1} \text{ yr}^{-1}$  at  $7.5^\circ \text{W}$  and  $3 \text{ m}^3 \text{ s}^{-1} \text{ km}^{-1} \text{ yr}^{-1}$  at  $6.5^\circ \text{W}$ . Considering the whole time period (1967–2007), the upwelling intensity suggests a positive trend with values around  $1 \text{ m}^3 \text{ s}^{-1} \text{ km}^{-1} \text{ yr}^{-1}$  at both points. Fig. 4(b) shows the variation in the number of days per year under upwelling favorable conditions ( $UI > 16 \text{ m}^3 \text{ s}^{-1} \text{ km}^{-1}$ ) from June to September at the 2 control points. Both points show a negative trend with values around  $-0.3 \text{ d yr}^{-1}$ . From these figures it is possible to observe the existence of interdecadal variations in upwelling conditions although the low statistical significance obtained (significance level  $< 90\%$ ) shows that the trend is not clear. The upwelling intensity and duration was also analyzed by means of the expression  $\sum_{i=1}^N n_i \langle UI \rangle_i^F$  where  $n_i$  is the number of consecutive days under upwelling favorable conditions considering  $n_i \geq 3$ ,  $\langle UI \rangle_i^F$  is the mean intensity of UI during these days and  $N$  is the number of events per year. Both control points show a negative trend although with a low significance level ( $< 90\%$ ). These results are in contradiction with those of Llope et al. (2006) who found a decreasing trend of  $-1.75 \text{ m}^3 \text{ s}^{-1} \text{ km}^{-1} \text{ yr}^{-1}$  in upwelling intensity and no change in the number of days under upwelling favorable conditions using an

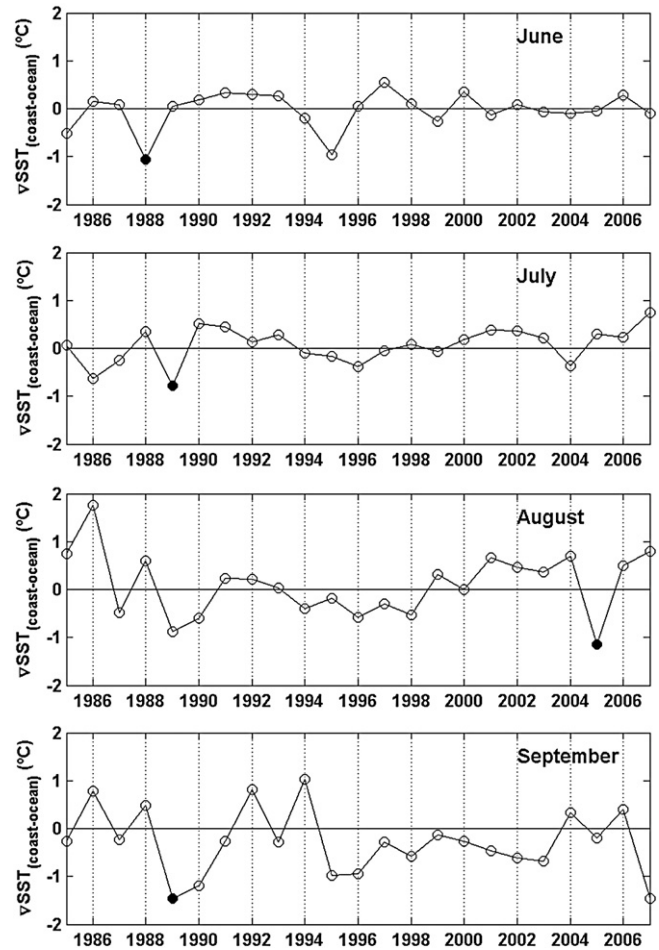


Fig. 5. Monthly SST difference between a coastal and ocean region spatially averaged in June, July, August and September. The coastal region corresponds to the area between the shoreline and the 200 m isobath (black line shown in Fig. 1(a)) and the ocean region to the area between  $44.5\text{--}45.5^\circ \text{N}$  and  $5.5\text{--}8.5^\circ \text{W}$ . Full circles refer to the extreme values observed for each summer month.

average of wind records from April to September, at the Asturias airport meteorological station from 1968 to 2003. This discrepancy can be due to the different period considered, the different position of the measurement point and the different source of wind data. It is necessary to take into account that wind data used by Llope et al. (2006) were measured at a land station where wind can be deflected by topographic features, while in the present work wind data are obtained from Sea Level Pressure fields over the ocean.

### 3.2. Water temperature analysis

Although the probability of upwelling events along the Cantabrian coast is considerably lower than along the Atlantic coast, upwelling events are still possible during summer months, being reflected in temperature changes both on the shelf and inside the estuaries.

#### 3.2.1. Offshore sea surface temperature

The presence of upwelled water at shelf can be analyzed in terms of  $\nabla\text{SST} = \text{SST}^{\text{coast}} - \text{SST}^{\text{ocean}}$  (Fig. 5), where the coastal region corresponds to the area between coast and 200 m isobath (black line shown in Fig. 1(a)) and the ocean region to the area between 44.5–45.5°N and 5.5–8.5°W. SST values were spatially averaged for the points inside these regions for every summer month (June–September) from 1985 to 2007. This gradient is similar to the Upwelling Index obtained using SST data (Nykjaer and Van Camp, 1994; Santos et al., 2005; deCastro et al., 2008b), which can be calculated as the SST gradient between coastal and oceanic locations at the same latitude. In

the present study, this gradient cannot be considered as an absolute Upwelling Index since temperature also changes with latitude due to differences in solar heating. However, it can provide an estimation of the presence of cold water near coast which can be related to upwelling events. In general,  $\nabla\text{SST}$  is close to zero (Fig. 5), which corresponds to neutral conditions without important upwelling events. Sharp negative peaks in the order of 1 °C correspond to years under strong upwelling favorable conditions. In particular, these events have been observed in June (1988 and 1995), July (1986 and 1989), August (1989 and 2005) and September (1989, 1990 and 2007). The full circles refer to the extreme values observed for each summer month.

The  $\nabla\text{SST}$  images shown in Fig. 6 correspond to those particular months (June 1988, July 1989, August 2005 and September 1989). Temperature gradients were calculated as the difference between SST at the month under study and the SST average calculated using the previous and following 2 years. Thus, for example Fig. 6(a) corresponds to the SST gradient between the situation observed in June 1988 and the average situation observed during the same month from 1986 to 1990. Voids correspond to cloud coverage. This procedure allows analyzing the behavior of the month under study with regard to the same month during the previous and following years in such a way that negative values near coast are linked to upwelling events. The observed results are independent of the averaging period although the chosen period ( $\pm 2$  years in this particular case) should be long enough to remove interannual oscillations and short enough to prevent the overlap of close negative peaks. In all frames, the most negative  $\nabla\text{SST}$  values, which range from  $-0.5$  to  $-1.0$  °C, are

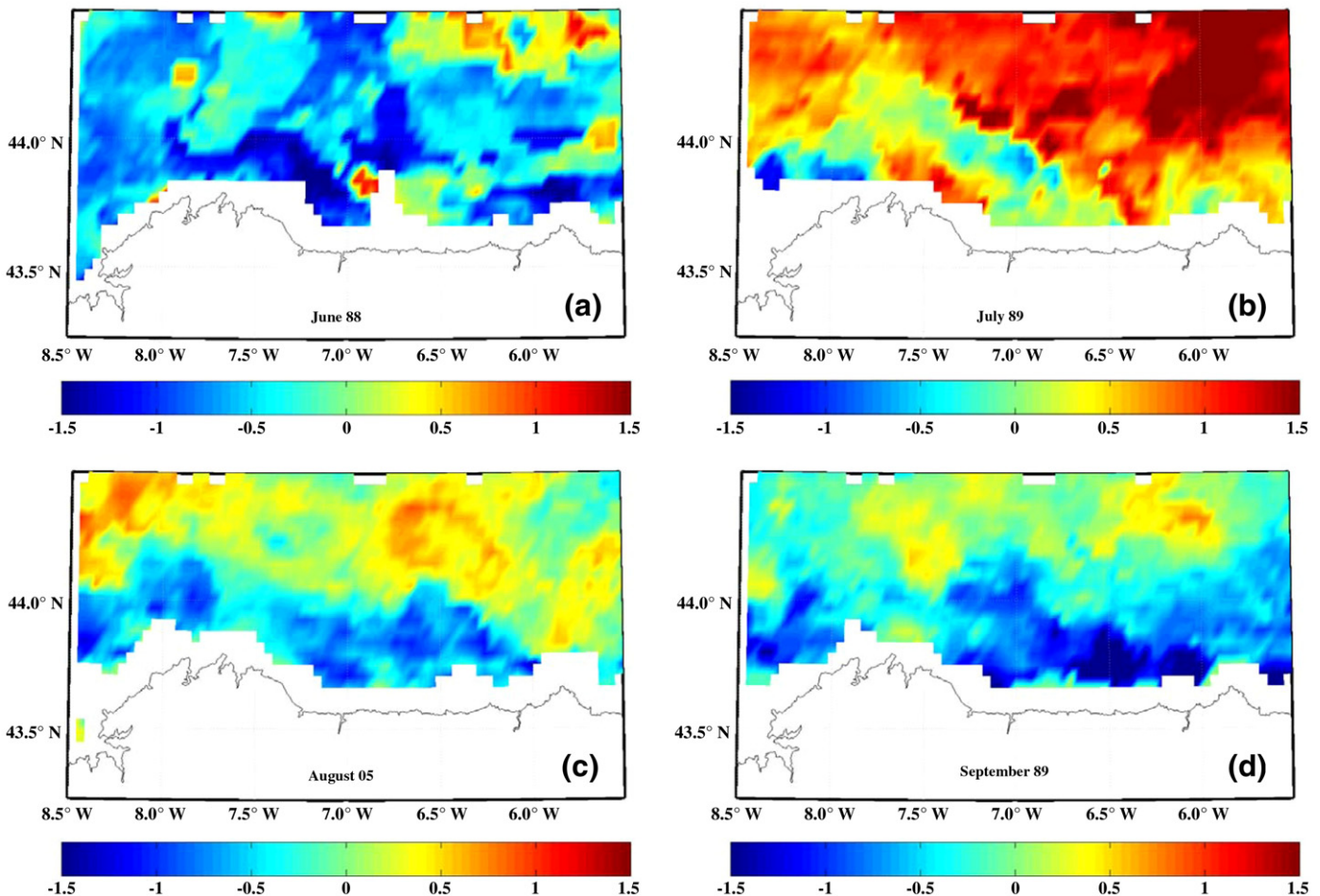


**Fig. 6.** Monthly SST images corresponding to the difference calculated between (a) June 1988 and the average situation observed in June from 1986 to 1990, (b) July 1989 and the average situation observed in July from 1987 to 1991, (c) August 2005 and the average situation observed in August from 2003 to 2007, (d) September 1989 and the average situation observed in September from 1987 to 1991.

**Table 2**

$\nabla$ SST calculated by  $SST^{\text{coast}} - SST^{\text{ocean}}$  corresponding to the particular months analyzed in Fig. 6 and UI averaged for these months at the 2 control points (6.5°W and 7.5°W) located in the central part of the area under study.

	$\nabla$ SST <sub>(coast-ocean)</sub> (°C)	UI ( $\text{m}^3 \text{s}^{-1} \text{km}^{-1}$ )	
Jun-88	-1.07	326 (6.5°W)	335 (7.5°W)
Jul-89	-0.78	284	262
Aug-05	-1.14	196	226
Sep-89	-1.45	302	304

observed over the shelf (the 200 m isobath is depicted in Fig. 1(a)) showing the existence of well developed upwelling events in the area. The spatial distribution of the upwelled water significantly differs between the 4 months under study. This could be due to the different wind conditions. Nevertheless, the atmospheric conditions observed for the particular months analyzed in this figure correspond to extreme positive upwelling indices ranging from 200 to  $300 \text{ m}^3 \text{ s}^{-1} \text{ km}^{-1}$  (Table 2). In addition, the upwelling favorable conditions (positive indices) were observed to last for more than 10 consecutive days during each month under study. This might indicate a complexity of upwelling events that is not resolved by the UI. Punctual upwelling events have been depicted by other authors (García-Soto et al., 2002) along the Cantabrian coast using AVHRR SST data. Here we have shown some of the most extreme events, which are characterized both by high intensity and long

duration. Thus, a permanent SST decrease on the order of  $1^\circ\text{C}$  has been observed to spread along the entire coastal area.

### 3.2.2. Estuarine temperature

Upwelling events along the Cantabrian coast have been studied by different authors (Botas et al., 1990; Prego and Bao, 1997) showing a temperature decrease at shelf. However, there is little evidence of upwelling inside the estuaries located in this area. Actually, only Alvarez et al. (2009) have shown the existence of upwelled water inside the northern Galician rias in winter.

Water temperature was measured at the inner part of one of the northern Galician rias (Ria de O Barqueiro) from June to September 2008 (Fig. 1(b), black diamond (st. B)).

The northern Galician rias are funnel-like incised valleys characteristic of a relatively submergent coastline with 30–35 m depth at their open mouths and around  $0.1 \text{ km}^3$  of water content. The Ria de O Barqueiro, as the rest of the northern Galician rias, lies on a mesotidal coast with a tidal range of 2–4 m and is dominated by marine processes except at the inner estuarine zone which is partially enclosed with well-developed beach barriers (Alvarez et al., 2009). The temperature recorder was placed in the intertidal part of the estuary in order to identify temperature changes induced by possible upwelling events where commercial species as oysters are cultured.

This monitoring has shown evidence of recurrent upwelling events in the area. The time evolution of the water temperature daily measured

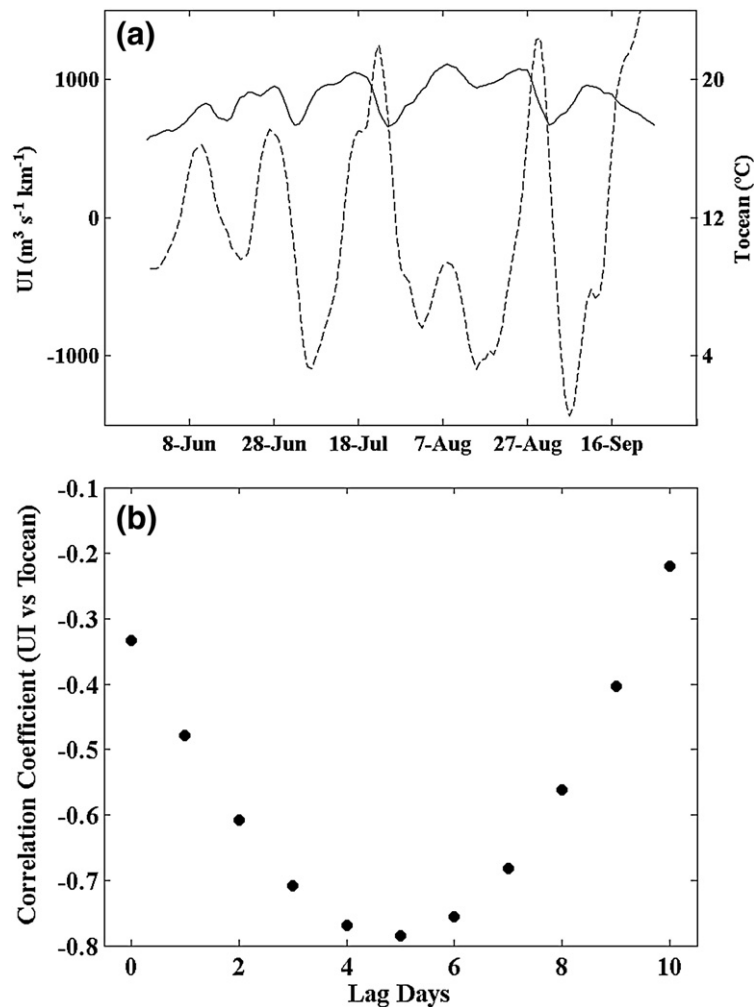


**Fig. 7.** (a) Temporal evolution of water temperature daily measured inside the Ria de O Barqueiro (Fig. 1(b), black diamond (st. B)) (black solid line) and temporal evolution of UI averaged at the 3 control points located in front of the northern Galician coast (Fig. 1(a), black circles) (black dashed line) from June to September 2008. (b) Lag correlation between the UI series and that of the water temperature shown in Fig. 7(a).

inside the ria is depicted in Fig. 7(a) (black solid line). Temperature signal shows a sequence between maxima and minima ranging from 17 °C to 21 °C. Note that the temperature axis range in the figure has been applied to easily identify the occurrence of the negative temperature peaks with regard to the positive UI peaks. UI was calculated at 3 control points located in front of the ria (Fig. 1(a), black circles) using QuikSCAT data to characterize the origin of this temperature variation. The average of the 3 points was calculated and represented in Fig. 7(a) (black dashed line). The UI signal also shows a sequence between maxima and minima. Maxima are related to easterly winds (upwelling favorable conditions) and minima to westerly winds. Taking into account the temporal evolution of temperature and UI signals, it is possible to observe that when a maximum occurs in UI, water temperature inside the ria shows a decrease a few days later. This behavior can be observed over the whole period showing evidence of different upwelling events which inject cold water from the ocean inside the ria. The correlation between UI and water temperature was calculated taking into account different lags between both variables (Fig. 7(b)). This correlation is negative because an increasing in UI implies a decreasing in water temperature. In addition, the correlation tends to increase as the number of lag days increases with the maximum value of  $-0.8$  (significance level  $>95\%$ ) corresponding to a lag of 5 days. The detected 5 days lag between the UI and the SST reaction shows that the effect of the wind pushing on the ocean surface has not an immediate response observable at the measuring point. It is a known fact that atmosphere–ocean interactions take place on a wide range of spatial and temporal scales. Nevertheless, taking into account that the control station was located at the inner part of the Ria de O Barqueiro (Fig. 1), the high lag could be due to the distance that the ocean upwelled water needs to cover to enter the ria until this point.

#### 4. Summary and conclusions

The occurrence and intensity of upwelling events have been characterized along the western part of the Cantabrian coast from 1967 to 2007. The UI showed a marked annual cycle with maximum values (upwelling favorable) in July–August and minimum ones in December–January. During the winter season, EA/WR and EA patterns explained the main variance of UI while during summer the UI variability was explained in terms of the EA pattern. The NAO pattern also showed some influence on UI.

The mean number of days under upwelling favorable conditions from June to September was around 12–14 days per month with a probability of finding these favorable conditions of  $\sim 17\%$  when events of at least 5 consecutive days were considered. SST data also revealed the presence of cold water near coast associated to upwelling favorable winds.

In addition, the analysis of the water temperature dependence on upwelling conditions in the inter-tidal area of the Ria de O Barqueiro from June to September 2008 showed that when a maximum UI occurs, water temperature inside the ria decreases a few days later. Both variables presented a negative correlation with the maximum value of  $-0.8$  corresponding to a lag of 5 days between them. The overall vertical velocity within the top layer results to be  $\langle w \rangle = Q_y/R_d$  where  $R_d$  is the Rossby radius. Taking into account that at this region  $R_d$  is about 12 km (Gil and Gomis, 2008) and considering  $Q_y = 0.3 \text{ m}^2\text{s}^{-1}$  (see Fig. 2(b), Section 3.1), it results  $\langle w \rangle \sim 2.5 \cdot 10^{-5} \text{ ms}^{-1}$ . The typical SST response time was estimated to be about 5 days, consequently the overall mixing (stirring) depth-scale results to be  $5 \text{ days} \cdot \langle w \rangle \sim 11 \text{ m}$ , a quite plausible value for the study area.

Finally, the present study has shown that intense and long lasting upwelling events can be observed over the western Cantabrian continental shelf although they are not as common as along the Atlantic coastline. This fact could provide favorable development conditions inside the estuaries for larval survival of IAS from warmer waters.

#### Acknowledgements

This work is supported by the Ministerio de Educacion y Ciencia under project CTM2007-62546-C03-03/MAR, by Xunta de Galicia under projects PGDIT06PXIB383285PR and PGDIT06PXIB383288PR and by the Dirección Xeral de Recursos da Consellería de Pesca e Asuntos Marítimos under project Estudio de viabilidade do cultivo de *crassostrea gigas* nas rias galegas. The first author of this work has been supported by the Fundação para a Ciência e a Tecnologia through a post-doctoral grant (SFRH/BPD/38292/2007).

#### References

- Alvarez, I., deCastro, M., Prego, R., Gomez-Gesteira, M., 2003. Hydrographic characterization of a winter-upwelling event in the Ria of Pontevedra (NW Spain). *Estuarine, Coastal and Shelf Science* 56, 869–876.
- Alvarez, I., deCastro, M., Gomez-Gesteira, M., Prego, R., 2005. Inter- and intra-annual analysis of the salinity and temperature evolution in the Galician Rias Baixas-ocean boundary (northwest Spain). *Journal of Geophysical Research* 110, C04008. doi:10.1029/2004JC002504.
- Alvarez, I., Gomez-Gesteira, M., deCastro, M., Novoa, E.M., 2008a. Ekman Transport along the Galician Coast (NW, Spain) calculated from QuikSCAT winds. *Journal of Marine Systems* 72, 101–115.
- Alvarez, I., Gomez-Gesteira, M., deCastro, M., Dias, J.M., 2008b. Spatio-temporal evolution of upwelling regime along the western coast of the Iberian Peninsula. *Journal of Geophysical Research* 113, C07020. doi:10.1029/2008JC004744.
- Alvarez, I., Ospina-Alvarez, N., Pazos, Y., deCastro, M., Bernardez, P., Campor, M.J., Gomez-Gesteira, J.L., Alvarez-Osorio, M.T., Gomez-Gesteira, M., Varela, M., Prego, R., 2009. A winter upwelling event in the Northern Galician Rias: frequency and oceanographic implications. *Estuarine, Coastal and Shelf Science* 82, 573–582. doi:10.1016/j.ecss.2009.02.023.
- Alvarez-Salgado, X.A., Gago, J., Miguez, B.M., Gilcoto, M., Perez, F.F., 2000. Surface waters of the NW Iberian Margin: upwelling on the shelf versus outwelling of upwelled waters from the Rias Baixas. *Estuarine, Coastal and Shelf Science* 51, 821–837.
- Alvarez-Salgado, X.A., Nieto-Cid, M., Gago, Brea, S., Castro, C.G., Doval, M.D., Perez, F.F., 2006. Stoichiometry of the degradation of dissolved and particulate biogenic organic matter in the NW Iberian upwelling. *Journal of Geophysical Research* 111 (C07017). doi:10.1029/2004JC002473.
- Bakun, A., 1973. Coastal upwelling indexes, west coast of North America, 1946–71. NOAA Technical Report, vol. 671. NMF, p. 103.
- Bode, A., Varela, M., Casas, B., Gonzalez, N., 2002. Intrusions of eastern North Atlantic central waters and phytoplankton in the north and northwestern Iberian shelf during spring. *Journal of Marine Systems* 36, 197–218.
- Borges, M.F., Santos, A.M.P., Crato, N., Mendes, H., Mota, B., 2003. Sardine Regime shifts off Portugal: a time series analysis of catches and wind conditions. *Scientia Marina* 67, 235–244.
- Botas, J., Fernandez, E., Bode, A., Anadon, R., 1990. A persistent upwelling off the Central Cantabrian Coast (Bay of Biscay). *Estuarine, Coastal and Shelf Science* 30, 185–199.
- Cabanas, J.M., Alvarez, I., 2005. Ekman transport patterns in the area close to the Galician coast (NW, Spain). *Journal of Atmospheric and Oceanographic Science* 10, 325–341.
- deCastro, M., Dale, A.W., Gomez-Gesteira, M., Prego, R., Alvarez, I., 2006a. Hydrographic and atmospheric analysis of an autumnal upwelling event in the Ria of Vigo (NW Iberian Peninsula). *Estuarine, Coastal and Shelf Science* 68, 529–537. doi:10.1016/j.ecss.2006.03.004.
- deCastro, M., Lorenzo, N., Taboada, J.J., Sarmiento, M., Alvarez, I., Gomez-Gesteira, M., 2006b. Teleconnection patterns influence on precipitation variability and on river flow regimes in the Miño River basin (NW Iberian Peninsula). *Climate Research* 32, 63–73.
- deCastro, M., Gomez-Gesteira, M., Alvarez, I., Cabanas, J.M., Prego, R., 2008a. Characterization of fall–winter upwelling recurrence along the Galician western coast (NW Spain) from 2000 to 2005: dependence on atmospheric forcing. *Journal of Marine Systems* 72, 145–148. doi:10.1016/j.jmarsys.2007.04.005.
- deCastro, M., Gomez-Gesteira, M., Lorenzo, M.N., Alvarez, I., Crespo, A.J.C., 2008b. Influence of atmospheric modes on coastal upwelling along the western coast of the Iberian Peninsula, 1985 to 2005. *Climate Research* 36, 169–179. doi:10.3354/cr00742.
- Fiuzza, A.F.G., 1984. Hidrologia e dinâmica das águas costeiras de Portugal (Hydrology and dynamics of the Portuguese coastal water). Ph.D. dissertation, 294 pp., Universidade de Lisboa, Lisboa.
- Fraga, F., 1981. Upwelling off the Galician Coast, Northwest Spain. In: Richardson, F.A. (Ed.), *Coastal Upwelling*. American Geophysical Union, Washington, pp. 176–182.
- García-Soto, C., Pingree, R.D., Valdes, L., 2002. Navidad development in the southern Bay of Biscay: climate change and swoddy structure from remote sensing and in situ measurements. *Journal of Geophysical Research* 107 (C8). doi:10.1029/2001JC001012.
- Gil, J., Gomis, D., 2008. The secondary ageostrophic circulation in the Iberian Poleward Current along the Cantabrian Sea (Bay of Biscay). *Journal of Marine Systems* 74, 60–73.
- Gomez-Gesteira, M., Moreira, C., Alvarez, I., deCastro, M., 2006. Ekman transport along the Galician coast (NW, Spain) calculated from forecasted winds. *Journal of Geophysical Research* 111 (C10005). doi:10.1029/2005JC003331.
- Lorenzo, M.N., Taboada, J.J., 2005. Influences of atmospheric variability on freshwater input in Galician Rias in winter. *Journal of Atmosphere and Ocean Sciences* 10, 377–387.



- Llope, M., Anadon, R., Viesca, L., Quevedo, M., Gonzalez-Quiros, R., Stenseth, N.C., 2006. Hydrography of the southern Bay of Biscay shelf-break region: integrating the multiscale physical variability over the period 1993–2003. *Journal of Geophysical Research* 111 (C09021). doi:10.1029/2005JC002963.
- Mann, R., Burreson, E.M., Baker, P.K., 1991. The decline of the Virginia oyster fishery in Chesapeake Bay: considerations for introduction of a non-endemic species, *Crassostrea gigas* (Thunberg, 1793). *Journal of Shellfish Research* 10, 379–388.
- Nykjaer, L., Van Camp, L., 1994. Seasonal and Interannual variability of coastal upwelling along northwest Africa and Portugal from 1981 to 1991. *Journal of Geophysical Research* 99 (C7), 14197–14207.
- Penabad, E., Alvarez, I., Balseiro, C.F., deCastro, M., Gomez, B., Perez-Muñuzuri, V., Gomez-Gesteira, M., 2008. Comparative analysis between operational weather prediction models and QuikSCAT wind data near the Galician coast. *Journal of Marine Systems* 72, 256–270.
- Prego, R., Bao, R., 1997. Upwelling influence on the Galician coast: silicate in shelf water and underlying surface sediments. *Continental Shelf Research* 17, 307–318.
- Prego, R., Guzmán-Zuñiga, D., Varela, M., deCastro, M., Gomez-Gesteira, M., 2007. Consequences of winter upwelling events on biogeochemical and phytoplankton patterns in a western Galician ria (NW Iberian peninsula). *Estuarine, Coastal and Shelf Science* 73, 409–422.
- Ríos, A.F., Pérez, F.F., Alvarez-Salgado, X.A., Figueiras, F.G., 1992. Water masses in the upper and middle North Atlantic Ocean east of the Azores. *Deep-Sea Research* 39, 645–658.
- Rodríguez-Puebla, C., Encinas, A.H., Nieto, S., Garmendia, J., 1998. Spatial and temporal patterns of annual precipitation variability over the Iberian Peninsula. *International Journal of Climatology* 18, 299–316.
- Ruiz, C., Abad, M., Sedano, F., García-Martín, L.O., Sánchez López, J.L., 1992. Influence of seasonal environmental changes on the gamete production and biochemical composition of *Crassostrea gigas* (Thunberg) in suspended culture in El Grove, Galicia, Spain. *Journal of Experimental Marine Biology and Ecology* 155, 249–262.
- Santos, A.M., Borges, M.F., Groom, S., 2001. Sardine and horse mackerel recruitment and upwelling off Portugal. *ICES Journal of Marine Science* 58, 589–596.
- Santos, A.M.P., Peliz, A., Dubert, J., Oliveira, P.B., Angelico, M.M., Re, R., 2004. Impact of a winter upwelling event on the distribution and transport of sardine (*Sardina pilchardus*) eggs and larvae off western Iberia: a retention mechanism. *Continental Shelf Research* 24, 149–165. doi:10.1016/j.csr.2003.10.004.
- Santos, A.M., Kazmin, A.S., Peliz, A., 2005. Decadal changes in the Canary upwelling system as revealed by satellite observations: their impact on productivity. *Journal of Marine Research* 63, 359–379.
- Shatkin, G., Shumway, S.E., Hawes, R., 1997. Considerations regarding the possible introduction of the Pacific oyster (*Crassostrea gigas*) to the Gulf of Maine: a review of global experience. *Journal of Shellfish Research* 16, 463–477.
- Torres, R., Barton, E.D., Miller, P., Fanjul, E., 2003. Spatial patterns of wind and sea surface temperature in the Galician upwelling region. *Journal of Geophysical Research* 108, 3130–3143. doi:10.1029/2002JC001361.